

¹⁸F-5-Fluoroaminosuberic Acid as a Potential Tracer to Gauge Oxidative Stress in Breast Cancer Models

Hua Yang¹, Silvia Jenni², Milena Colovic^{1,3}, Helen Merkens², Carlee Poleschuk¹, Isabel Rodrigo¹, Qing Miao¹, Bruce F. Johnson⁴, Michael J. Rishel⁴, Vesna Sossi⁵, Jack M. Webster⁴, François Bénard^{2,3}, and Paul Schaffer^{1,3,6}

¹Life Sciences, TRIUMF, Vancouver, Canada; ²British Columbia Cancer Agency, Vancouver, Canada; ³Department of Radiology, University of British Columbia, Vancouver, Canada; ⁴GE Global Research, Niskayuna, New York; ⁵Department of Physics and Astronomy, University of British Columbia, Vancouver, Canada; and ⁶Department of Chemistry, Simon Fraser University, Vancouver, Canada

The cystine transporter (system x_C^-) is an antiporter of cystine and glutamate. It has relatively low basal expression in most tissues and becomes upregulated in cells under oxidative stress (OS) as one of the genes expressed in response to the antioxidant response element promoter. We have developed ¹⁸F-5-fluoroaminosuberic acid (FASu), a PET tracer that targets system x_C^- . The goal of this study was to evaluate ¹⁸F-FASu as a specific gauge for system x_C^- activity in vivo and its potential for breast cancer imaging. **Methods:** ¹⁸F-FASu specificity toward system x_C^- was studied by cell inhibition assay, cellular uptake after OS induction with diethyl maleate, with and without anti-xCT small interfering RNA knockdown, in vitro uptake studies, and in vivo uptake in a system x_C^- -transduced xenograft model. In addition, radiotracer uptake was evaluated in 3 breast cancer models: MDA-MB-231, MCF-7, and ZR-75-1. **Results:** Reactive oxygen species-inducing diethyl maleate increased glutathione levels and ¹⁸F-FASu uptake, whereas gene knockdown with anti-xCT small interfering RNA led to decreased tracer uptake. ¹⁸F-FASu uptake was robustly inhibited by system x_C^- inhibitors or substrates, whereas uptake was significantly higher in transduced cells and tumors expressing xCT than in wild-type HEK293T cells and tumors ($P < 0.0001$ for cells, $P = 0.0086$ for tumors). ¹⁸F-FASu demonstrated tumor uptake in all 3 breast cancer cell lines studied. Among them, triple-negative breast cancer MDA-MB-231, which has the highest xCT messenger RNA level, had the highest tracer uptake ($P = 0.0058$ when compared with MCF-7; $P < 0.0001$ when compared with ZR-75-1). **Conclusion:** ¹⁸F-FASu as a system x_C^- substrate is a specific PET tracer for functional monitoring of system x_C^- and OS imaging. By enabling noninvasive analysis of x_C^- responses in vivo, this biomarker may serve as a valuable target for the diagnosis and treatment monitoring of certain breast cancers.

Key Words: oxidative stress; system x_C^- ; PET; tumor imaging; F-18

J Nucl Med 2017; 58:367–373

DOI: 10.2967/jnumed.116.180661

Oxidative stress (OS) is the result of an imbalance in cellular reactive oxygen species and antioxidants, and the cellular response to OS has been recognized as a critical regulatory mechanism for

cancer and cancer stem cells (1,2). During OS, the expression of antioxidant response-regulated genes, including the key subunit of the x_C^- cystine transporter system (xCT, *SLC7A11*), are upregulated through the KEAP1-Nrf2 pathway (3), which leads to increased biosynthesis of glutathione. Glutathione is the predominant endogenous cellular antioxidant and plays a critical role in the defensive cellular response to OS by neutralizing free radicals and reactive oxygen and nitrogen compounds (4,5). The rate-limiting precursor for glutathione synthesis is cysteine, which cells can obtain through uptake of its oxidized form, cystine. System x_C^- plays its primary role by importing cystine to provide cysteine for glutathione synthesis in response to OS. In addition, x_C^- serves as a mediator of physiologic redox potential across the cell membrane, working in concert with other transporters to establish an appropriate level of cystine/cysteine on both sides of the cell membrane (4). System x_C^- transporter activity and expression in normal cells is typically low but is significantly upregulated in cells under OS (6). Thus, x_C^- transporter activity is a promising platform from which to develop targeted treatments for cancer, with several groups exploring the feasibility of targeting the unique x_C^- subunit, xCT, for cancer therapeutics (7–12). Tumors with increased xCT activity are associated with resistance to chemotherapy, and inhibition of xCT has been shown to sensitize cancer cells to chemotherapeutic drugs such as doxorubicin (12,13), gemcitabine, celastrol (14), and etoposide (15). In addition, immunohistochemical analysis of xCT protein expression has been shown to correlate with tumor staging (16). Consequently, the x_C^- transporter may be a useful diagnostic target for cancer imaging, and using this transporter as a functional reporter of OS may provide valuable information for clinical cancer management, including early detection, staging, patient stratification, monitoring of response to therapy, and development of new therapeutics.

We developed a cystine/glutamate analog, ¹⁸F-5-fluoro-aminosuberic acid (FASu), as a potent cystine transporter substrate with the goal of assessing its potential as a diagnostic tracer of OS via x_C^- activity (17). We previously reported the design, synthesis, and in vivo evaluation of ¹⁸F-¹⁸F-FASu in EL4 and SKOV3 tumor models (17). Our previous study on ¹⁸F-FASu demonstrated high tumor-to-background ratios in both tumor types, prompting us to evaluate the specificity of this tracer for xCT and its potential utility in the detection and monitoring of other tumor types. Herein we report the in vitro and in vivo studies that establish ¹⁸F-FASu uptake via system x_C^- in 3 breast cancer models. Our studies include MCF-7, ZR-75-1, and a triple-negative breast cancer model, MDA-MB-231, representing a range of breast cancer subtypes. We are particularly

Received Jul. 11, 2016; revision accepted Nov. 7, 2016.
For correspondence or reprints contact: Paul Schaffer, Life Sciences, TRIUMF, 4004 Westbrook Mall, Vancouver, Canada, V6T 2A3.
E-mail: pschaffer@triumf.ca
Published online Oct. 27, 2016.
COPYRIGHT © 2017 by the Society of Nuclear Medicine and Molecular Imaging.

interested in triple-negative breast cancer, which maintains low expression levels of estrogen receptor, progesterone receptor, and human epidermal growth factor receptor 2 and is typically associated with poor patient outcomes, including lower overall survival rates as well as aggressive and early recurrence (18). The cystine transporter is commonly expressed and functional in triple-negative breast cancer, and inhibition with sulfasalazine can increase reactive oxygen species and slow cell growth in MDA-MB-231 tumors (8). An exploratory clinical study with ^{18}F -(4*S*)-4-(3- ^{18}F -fluoropropyl)-L-glutamate, a glutamate analog that targets system x_C^- , showed significant uptake in a subset of breast cancer lesions (19). The purpose of this study was to evaluate the relationship between system x_C^- and ^{18}F -FASu uptake in models of human breast cancer.

MATERIALS AND METHODS

Radiosynthesis of ^{18}F -FASu

Radiosyntheses were performed on a TRACERlab FXFN module (GE Healthcare) in a lead-shielded hot cell using our reported method (17). Reverse-phase high-performance liquid (HPLC) chromatography was carried out on an Agilent 1200 series system equipped with a diode array detector and a Raytest GABI Star scintillation detector using a Phenomenex Monolithic C_{18} 4.6 \times 100 mm column. Chemicals and reagents were purchased from Sigma Aldrich, Acros Organics, and Fisher Scientific. Radiofluorination $^{18}\text{F}^-$ was produced in a TR13 cyclotron from bombardment of H_2^{18}O at 20 μA . The produced $\text{H}_2^{18}\text{O}/^{18}\text{F}^-$ was delivered to an FXFN automated synthesis module, where the $^{18}\text{F}^-$ was trapped on a QMA resin. The resin was purged with helium, and the fluoride was subsequently released using a mixture of Kryptofix[2.2.2] (10.1 mg in 200 μL of acetonitrile) and K_2CO_3 (2.1 mg in 200 μL of water). The solvent was removed by the repeated volatilization of acetonitrile (1.5 mL) under reduced pressure. The precursor (di-tert-butyl 2-((bis-tert-butoxycarbonyl)amino)-5-(tosyloxy)octanedioate, compound **1**, Fig. 1), 1.4 mg, was previously dried in vacuo and dissolved in 500 μL of anhydrous dimethyl sulfoxide in preparation for labeling. The precursor was added to Kryptofix[2.2.2]/ $^{18}\text{F}^-$, and the reaction was heated at 95°C for 20 min, after which the reaction mixture was cooled to 35°C, diluted by 7 mL of H_2O , and then loaded onto a Waters tC18 Plus Sep-Pak. The Sep-Pak was washed with 17 mL of distilled, deionized H_2O , and di-tert-butyl 2-((bis-tert-butoxycarbonyl)amino)-5-fluorooctanedioate (compound **2**, Fig. 1) was eluted using 1.5 mL of acetonitrile. In a separate apparatus, the solvent was removed under the flow of N_2 at 95°C. Trifluoroacetic acid (500 μL) and anisole (8 μL) were added, and the mixture was heated at 95°C for 7 min. After trifluoroacetic acid was removed in vacuo, the residue was dissolved in 0.6 mL of phosphate-buffered saline and then passed through a Waters tC18 light Sep-Pak. The Sep-Pak was washed with an additional 0.6 mL of phosphate-buffered saline. The combined phosphate-buffered saline solution that contained ^{18}F -FASu was filtered through a 0.22- μm membrane to generate the final product. Decay-corrected radiochemical yield was 18% \pm 6% ($n = 6$), radiochemical purity was more than 98%, and specific activity

was 17.5 \pm 7 GBq/mmol ($n = 6$). The identities of compound **2** and ^{18}F -FASu were confirmed by HPLC comparison with the standards.

Quality control of the radiosynthesis was performed by ultraviolet and radio-HPLC. The chromatograms are shown in Supplemental Figure 1. The retention time difference between ^{18}F -FASu and FASu was 0.27 min, in line with the delay between the ultraviolet detector and the γ -detector.

The HPLC method was as follows: Phenomenex Monolithic C18 column, 100 mm \times 4.6 mm, 1 mL/min; A: 0.1% trifluoroacetic acid in H_2O , B: 0.1% trifluoroacetic acid in acetonitrile; gradient flow from 100% A at 0 min to 20% A and 80% B in 15 min.

In Vivo and In Vitro Stability Studies

For the serum stability study, 0.74 MBq of ^{18}F -FASu in 10 μL of phosphate-buffered saline was incubated with 100 μL of Rag2M plasma for 5, 15, 30, 45, 60, 90, and 120 min. After each incubation, the sample was centrifuged through a membrane with a molecular weight cutoff of 10 kDa (Microcon, 145,000 rpm; Millipore) and analyzed by HPLC. No degradation was observed until 60 min. At 90 min, a small shoulder peak (20%) appeared. At 120 min, the same shoulder peak was observed at 27% compound to primary product peak.

For in vivo stability studies, urine and blood samples were collected from two Rag2M mice at 10 and 60 min after injection. The blood samples were centrifuged to collect the serum. Both serum and urine were passed through a 10-kDa membrane to remove protein, followed by HPLC analysis. No metabolites were observed for urine samples at 10 or 60 min. For the blood samples, no degradation was present at 10 min, and 15.5% \pm 0.5% degradation was observed at 60 min.

Cell Culture and Uptake Experiments

The HEK-293T cell line was purchased from Clontech Laboratories. The ZR-75-1 cell line was purchased from ATCC. The MCF-7 cell line was obtained as a gift from Dr. C. Kent Osborne (Baylor College of Medicine) and authenticated by DDC Medical. The MDA-MD-231 cell line was obtained as a gift from Dr. Connie Eaves and authenticated by DDC Medical.

The MDA-MB-231 cell line was cultured in complete Dulbecco modified Eagle medium (with 4,500 mg/L glucose + 10% fetal bovine serum + 1% penicillin/streptomycin). ZR-75-1 was cultured in complete RPMI-1640 (with 10% fetal bovine serum + 1% penicillin/streptomycin). MCF-7 was cultured in complete Dulbecco modified Eagle medium with 1% minimum-essential-medium nonessential amino acid solution. Cells were maintained in 10-cm tissue culture dishes in a humidified incubator at 37°C with 5% CO_2 and routinely subcultured at approximately 95% confluency.

For uptake studies, cells were seeded into 24-well plates (1 \times 10⁵ cells/mL) such that confluency was achieved the next day. Each plate was washed 3 times with cold HEPES (4-(2-hydroxyethyl)-1-piperazineethanesulfonic acid)-Hanks balanced salt solution, and then 0.148 MBq of ^{18}F -FASu in 400 μL of HEPES-Hanks balanced salt solution was added. Cell numbers were established from a single well using a Moxi Z Mini Automated Cell Counter (Orflo Technologies).

Subsequently, the samples were incubated at 37°C with orbital shaking for the indicated duration. After incubation, supernatants were removed, cells were washed twice with cold HEPES-Hanks balanced salt solution, 400 μL of 1 M NaOH were added to the cells, the NaOH lysate was collected 10 min later, and 25 μL of the lysate was taken to assess the protein concentration using a Pierce bicinchoninic acid protein assay kit (Thermo

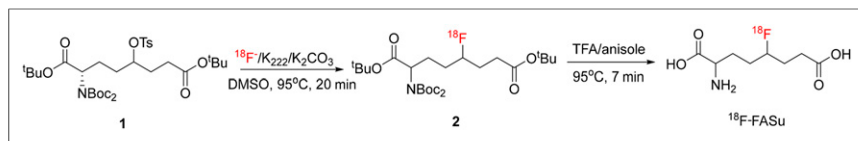


FIGURE 1. Radiosynthesis of ^{18}F -FASu. DMSO = dimethyl sulfoxide; TFA = trifluoroacetic acid.

Fisher Scientific). The activity in the solution and lysate was measured using a PerkinElmer Wizard 2480 γ -counter and normalized to the protein concentration.

For diethyl maleate (DEM)-induced OS experiments, DEM was added at various concentrations approximately 24 h before harvesting. The uptake study was conducted using the method described above.

For amino acid transporter inhibition experiments, all chemicals were purchased from Sigma-Aldrich and used without further modification. L-Glu, D-Asp, 2-amino-2-norbornanecarboxylic acid (BCH), L-Leu, and L-Ser were used at a 2 mM concentration, and sulfasalazine was used at a 1.0 mM concentration. The inhibitors were added to MDA-MB-231 cells and incubated with ^{18}F -FASu at 37°C with 5% CO_2 for 60 min.

Small Interfering RNA (siRNA) Knockdown Experiments

MDA-MB-231 cells were seeded at 1×10^5 cells/mL in a 24-well plate with complete Dulbecco modified Eagle medium 24 h before transfection with siRNA (xCT siRNA and nontargeting control siRNA, both from Santa Cruz Biotechnologies). Cells were transfected at 80% confluency with a mixture containing 25 nM siRNA, 1.5 μL of TransitIT siQuest transfection reagent (Mirus), and Opti-MEM reduced serum medium (Life Technologies) prepared and added according to the manufacturers' directions. The cells were left to incubate at 37°C with 5% CO_2 for 24 h. Then, 0.1 mM DEM was added to the cells and incubated an additional 24 h, followed by a tracer uptake study using the method described above.

Glutathione Quantification

Glutathione content was determined, in triplicate, using the Thiol Detection Assay Kit from Cayman Chemical per the manufacturer's instructions. The fluorescent signal was recorded using a FlexStation 3 spectrophotometer (Molecular Devices). The glutathione content in each sample was estimated from the standard curve and normalized to protein content.

HEK::xCT Cell Line

The lentiviral plasmid Lv205 (pReceiver-ORF-IRES-eGFP-IRES-Puro) containing the open reading frame of human *SLC7A11* (GeneCopoeia) was used to generate virus particles using a second-generation packaging system. HEK-293T cells grown in antibiotic-free medium were transduced using 3:1 plasmids (Lv205-xCT and the packaging plasmids) to the transduction reagent ratio following the manufacturer's instructions (transit-LT1; Mirus) and incubated at 37°C. The cell culture supernatant containing the virus was harvested 48 and 72 h after the transduction, passed through a 0.45- μm low-protein binding filter, and directly incubated on HEK-293T cells grown to 50% confluency. After 48 h of incubation, cells were passaged 3 times with complete medium before those harboring the xCT-plasmid were selected by adding puromycin at 3 $\mu\text{g}/\text{mL}$.

The green fluorescent protein tag of HEK::xCT allows confirmation of the expression of xCT using confocal microscopy. The green fluorescent protein and normal image overlay are shown in Supplemental Figure 2 (supplemental materials are available at <http://jnm.snmjournals.org>).

Quantitative Polymerase Chain Reaction (PCR)

Transcriptional expression of xCT (*SLC7A11*) in MDA-MB-231, MCF-7, and ZR-75 cells was determined relative to hypoxanthine phosphoribosyltransferase 1 (*HPRT1*). Total RNA was purified using the GenElute Mammalian Total RNA Miniprep Kit (Sigma), treated with amplification grade DNase I (Sigma), and measured using a NanoDrop spectrophotometer. A 50-ng quantity of total RNA from each sample was reverse-transcribed in a 20- μL reaction using a SuperScript VILO cDNA synthesis kit (Invitrogen). Quantitative PCR was set up in 384-well plates and performed on a QuantStudio

6K Flex Real-Time PCR system. Each 10- μL reaction contains 1 μL of template cDNA, 500 μM forward and reverse primers, 250 μM probe (IDT), and $1 \times$ SsoAdvanced Universal Probes Supermix (Bio Rad). MDA-MB-231 was assayed in triplicate; MCF-7 and ZR-75 were assayed in 2 \times triplicate. The concentration of each target was determined by interpolating the threshold cycle value from respective standard curves of known concentrations.

The IDT PrimeTime quantitative PCR primers were Hs.PT.58.38930943 for *SLC7A11* and Hs.PT.58v.45621572 for *HPRT1*.

To construct the *SLC7A11* and *HPRT1* standard curves, total RNA from MDA-MB-231 cells was purified and reverse-transcribed, and *SLC7A11* and *HPRT1* genes were amplified using the same primers as for the quantitative PCR reaction and Q5 High-Fidelity DNA polymerase (New England BioLabs) per the manufacturer's instructions. PCR products were separated on a 2% agarose gel, and target bands were extracted. The DNA was purified using the Monarch DNA Gel Extraction Kit (New England BioLabs) and quantified using the Qubit dsDNA HS assay kit (Thermo Fisher). Standard curves were constructed using 10-fold serial dilutions and assayed by quantitative PCR in triplicate (Supplemental Fig. 3).

Small-Animal PET and Biodistribution Studies

All animal experiments were conducted in accordance with the guidelines established by the Canadian Council on Animal Care and approved by the Animal Care Committee of the University of British Columbia. Female immunodeficient RAG2M mice (12–14 wk, 19–26 g) were obtained from an in-house breeding colony at the Animal Resource Centre of the British Columbia Cancer Research Centre.

MDA-MB-231, ZR-75-1, MCF-7, and HEK-293T tumors were inoculated subcutaneously with 5–10 $\times 10^6$ cells in Matrigel (Corning) on the dorsal flank of the mice. MCF-7 and ZR-75-1 required implantation of a 17β -estradiol releasing pellet (0.36 mg/60 d, Innovative Research of America) 7 d before inoculation.

Once palpable tumors measuring about 7–10 mm were obtained (~2–4 wk), the mice were anesthetized by 2% isoflurane inhalation and intravenously injected with about 3.7 MBq of ^{18}F -FASu. The activity in the syringe was counted before and after injection to determine the exact injected dose.

For blocking experiments, the radiotracer was coinjected with a 100 mg/kg dose of nonradioactive aminosuberic acid. After the injections, the mice were allowed to recover and roam freely in their cages for 60 min. The animals were then anesthetized by 2% isoflurane inhalation and euthanized by CO_2 at various time points. Blood was promptly withdrawn via a cardiac puncture, and the tissues of interest were harvested, rinsed in phosphate-buffered saline, blotted dry, and weighed. The radioactivity of the collected mouse tissues was counted on a γ -counter and expressed as the percentage injected dose per gram of tissue (%ID/g).

Mice destined for a static emission scan were anesthetized with 2% isoflurane inhalation 1 or 2 h after intravenous injection of the tracer and placed on the scanner. A baseline CT scan was obtained for localization and attenuation correction. During the acquisition, anesthesia was maintained and the mice were kept warm with a heating pad. A single static emission scan was acquired for 15 min. Afterward, the mice were euthanized and the organs harvested for biodistribution as described above.

Statistical Analysis

Test statistics and *P* values were calculated using Minitab Express analysis software. The descriptive statistics are reported as mean \pm SD when applicable. Means were compared using a 2-sample *t* test, assuming equal variance. A *P* value of less than 0.05 was considered significant.

TABLE 1

¹⁸F-FASu Uptake in MDA-MB-231 in Presence of Common Amino Acid Transporter Substrates and Inhibitors (n = 4)

Parameter	D-Asp	L-Leu	L-Ser	BCH	L-Glu	L-ASu	SSZ	Control
Transporter	EAAT	L, B ⁰ , B ⁰⁺	A, ACS, B ⁰ , B ⁰⁺	L	x _C ⁻ , EAAT, VGLUT	x _C ⁻	x _C ⁻	—
Uptake (%)	119 ± 18	111 ± 13	126 ± 14	115 ± 15	24 ± 3	25 ± 3	14 ± 2	100%
P	0.0615	0.1122	0.0043	0.0597	<0.0001	<0.0001	<0.0001	—

SSZ = sulfasalazine; EAAT = excitatory amino acid transporter.

RESULTS

In Vitro Uptake Specificity Studies

To examine the uptake specificity of ¹⁸F-FASu in cancer cell lines, we studied tracer uptake in the triple-negative breast cancer cell line MDA-MB-231 at 60 min in the presence of substrates or inhibitors of common amino acids (Table 1). The results showed no statistically significant difference between uptake with and without D-Asp, L-Leu, or BCH, whereas uptake increased to 126% ± 14% in the presence of L-Ser, indicating uptake is not through excitatory amino acid transporters, system L, B⁰, B⁰⁺, A, or ACS. Tracer uptake was suppressed only by L-Glu, L-ASu, and sulfasalazine, all of which are substrates or inhibitors of system x_C⁻, indicating that among the transporters analyzed here, uptake of ¹⁸F-FASu is specific to system x_C⁻.

It has been reported that DEM, as an electrophilic oxidant, induces xCT expression and concomitantly increases cellular glutathione levels (20–22). Cellular uptake of ¹⁸F-FASu showed a dose-dependent increase after DEM incubation (Fig. 2A). The uptake gradually increased with the addition of 2, 5, 10, and 20 μM DEM

and plateaued at a higher concentration. Cellular glutathione levels showed a similar trend over the same DEM concentration range (Fig. 2B). These results indicate that with increased OS inducer, higher levels of glutathione are maintained, which correlates with higher tracer uptake. In contrast, when system x_C⁻ was knocked down on incubation with xCT siRNA, ¹⁸F-FASu uptake decreased significantly compared with the cells incubated with nontargeting control siRNA (62% ± 5%, P = 0.0017) or without siRNA (68% ± 3%, P = 0.0010, Fig. 2C).

Between the 2 subunits of system x_C⁻, xCT is unique to system x_C⁻, leading us to establish a positive control cell line by transducing HEK293T (HEK wild-type) cells with an xCT expression vector (HEK::xCT). The cell uptake of ¹⁸F-FASu at 1 h in HEK::xCT cells was 5.4 ± 0.5 × 10⁴ cpm/10⁵ cells, whereas the uptake in wild-type cells was only 6.5 ± 1.1 × 10³ cpm/10⁵ cells (P < 0.0001, Fig. 2D) under the same conditions.

In Vivo Uptake Specificity Study in xCT Transduced Tumor Xenograft

A biodistribution study was also performed using female mice inoculated with both HEK::xCT and HEK wild-type tumors. The average tumor uptake was 10.4 ± 4.1 %ID/g (n = 5) for HEK::xCT and 4.0 ± 0.6 %ID/g (n = 5) for HEK wild-type (Fig. 3A). Both tumors exhibited lower uptake when coinjected with aminosuberic acid as a blocking agent (Fig. 3A). HEK::xCT uptake decreased by 67% (n = 3), whereas the HEK wild-type tumor saw a 54% decline (n = 3). Figure 3B shows a static PET image acquired at 1 h after injection, which confirmed higher uptake in HEK::xCT and lower uptake in HEK wild-type. In addition to tumor, kidneys (11.2 ± 4.9 % ID/g), and bladder, appreciable uptake was also observed in pancreas (18.0 ± 2.8 %ID/g), spleen (3.4 ± 1.3 %ID/g), ovaries (4.3 ± 2.6 %ID/g), and uterus (4.1 ± 3.9 %ID/g), all of which decreased with coinjection of aminosuberic acid. Uptake in blood (0.43 ± 0.11 %ID/g) and muscles (0.17 ± 0.02 %ID/g) was much lower than in tumors.

Human Breast Cancer Cell Line In Vitro Data

MDA-MB-231, MCF-7, and ZR-75-1 have modest to low reported xCT messenger RNA expression among the breast cancer cell lines (23). We measured the copy number of *SLC7A11* (xCT) transcripts in MDA-MB-231, MCF-7 and ZR-75-1 cell lines using absolute quantitative PCR (Fig. 4B). MDA-MB-231 cells expressed the highest *SLC7A11* level of the 3 cell lines (842 ± 45 copies/μL for MDA-MB-231, 237 ± 80 copies/μL for MCF-7, and 314 ± 54 copies/μL for ZR-75-1). Uptake of ¹⁸F-FASu in the cells increased over 60 min (Fig. 4A). MDA-MB-231 had the highest uptake of the 3 cell lines, whereas MCF-7 had the lowest uptake over 60 min. This is consistent with the trend in messenger

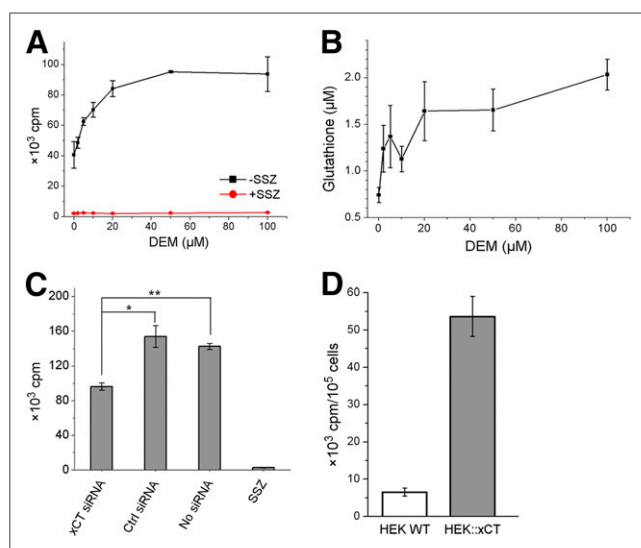


FIGURE 2. ¹⁸F-FASu uptake specificity study. (A) ¹⁸F-FASu uptake in MDA-MB-231 cells at 60 min with addition of DEM at 0, 2, 5, 10, 20, 50, and 100 μM to induce OS. (B) Glutathione concentration in MDA-MB-231 cells with addition of DEM at 0, 2, 5, 10, 20, 50, and 100 μM. (C) Uptake in MDA-MB-231 cells after addition of xCT siRNA, control siRNA, no siRNA, or 500 μM sulfasalazine. (D) Uptake in HEK wild-type and HEK::xCT cells at 60 min (P < 0.0001). *P = 0.0017. **P = 0.0010. SSZ = sulfasalazine.

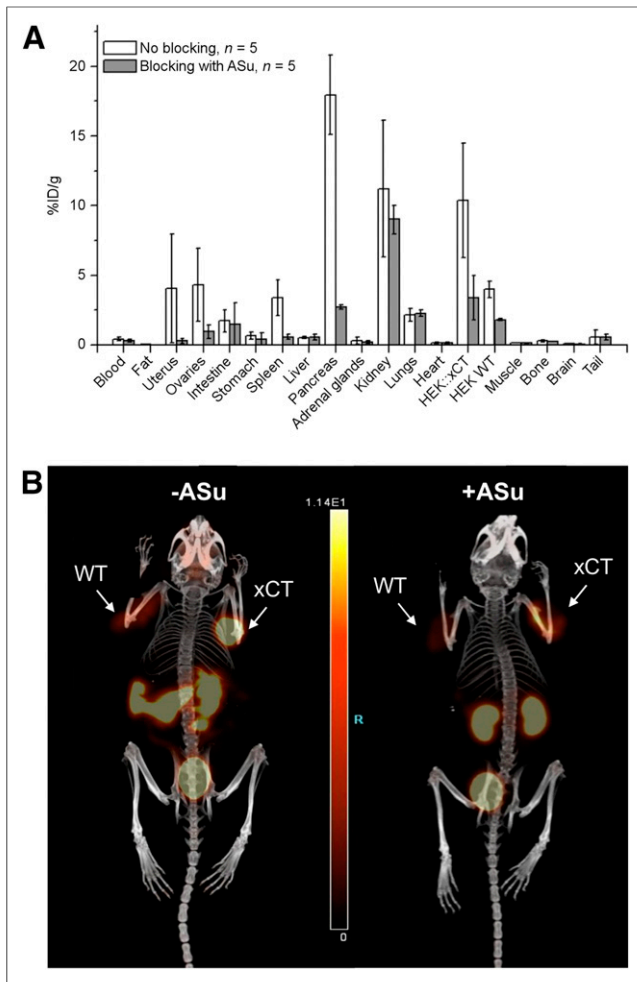


FIGURE 3. (A) Biodistribution with ($n = 5$) and without ($n = 5$) coinjection of 100 mg/kg dose of aminosuberic acid in mice bearing both HEK::xCT and HEK wild-type tumors. (B) PET maximum-intensity projection at 45–60 min after injection. Kidneys and bladder are visible on both images, whereas pancreas and spleen are visible only in unblocked condition. WT = HEK wild-type tumor; xCT = HEK::xCT tumor.

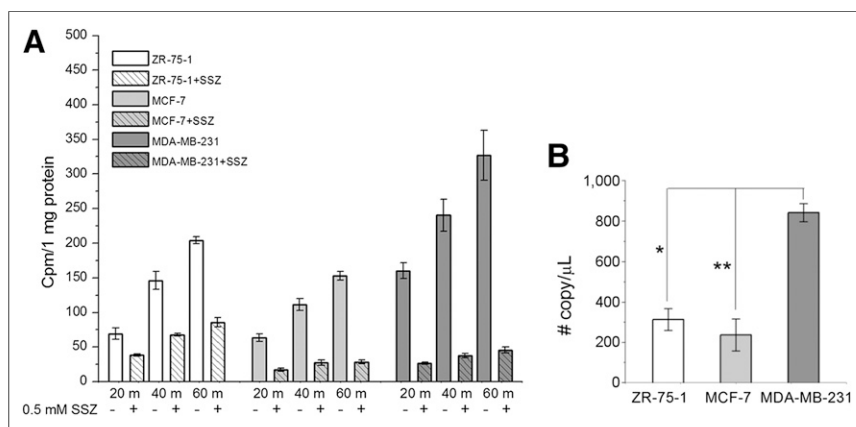


FIGURE 4. (A) ^{18}F -FASu uptake in MDA-MB-231, MCF-7, and ZR-75-1 cell lines at 20, 40, and 60 min with and without system x_C^- inhibitor sulfasalazine (0.5 mM). (B) xCT messenger RNA expression levels in ZR-75-1, MCF-7, and MDA-MB-231 cells. * $P < 0.0001$. ** $P < 0.0001$. SSZ = sulfasalazine.

RNA expression level measured. For MDA-MB-231 and MCF-7, uptake was suppressed by $86\% \pm 13\%$ and $82\% \pm 9\%$ ($n = 4$), respectively, by adding the system x_C^- inhibitor sulfasalazine, whereas uptake in ZR-75-1 was suppressed by only $58\% \pm 5\%$ ($n = 4$) with sulfasalazine, indicating that ZR-75-1 cells may exhibit an alternative, unknown, uptake mechanism.

Human Breast Cancer Tumor Xenograft In Vivo Data

In vivo MDA-MB-231 tumor uptake in RAG2M mice at 5, 30, 60, and 120 min after injection was studied. The tumor-to-blood ratio continuously increased to 7.2 at 120 min (Fig. 5A). The tumor-to-muscle ratio increased to 8.1 at 60 min and remained at this level through 120 min after injection. The PET imaging results at 2 h after injection, along with the biodistribution analysis of ^{18}F -FASu in MDA-MB-231 tumor-bearing mice, are shown in Figures 5B and 5C. The highest organ uptake was in pancreas, probably because of the high xCT level in this organ (24). The kidneys also had high uptake, suggesting a preference of renal clearance for this radiotracer. Other organs exhibiting high uptake included spleen, uterus, and ovaries, which are also reported to have relatively higher levels of xCT expression (25).

At 2 h after injection, uptake in MDA-MB-231, MCF-7 and ZR-75-1 tumors was $1.38 \pm 0.27\% \text{ID/g}$ ($n = 9$), $1.01 \pm 0.20\% \text{ID/g}$ ($n = 8$), and $0.75 \pm 0.14\% \text{ID/g}$ ($n = 8$), respectively (Fig. 5D). Whole-body biodistribution is shown in the supplemental data. Uptake in MDA-MB-231 tumors was higher than in ZR-75-1 or MCF-7 tumors ($P < 0.0001$ when compared with ZR-75-1, $P = 0.0058$ when compared with MCF-7), consistent with the higher messenger RNA expression level measured in MDA-MB-231 cells.

DISCUSSION

Clinical functional imaging in oncology has long relied on the analysis of enhanced glucose utilization—as monitored by ^{18}F -FDG—for tumor detection. The success of ^{18}F -FDG is due, in part, to the fact that it is a substrate for a ubiquitous cellular pathway and holds relevance for a wide number of clinical indications. OS is a common pathogenic process in many diseases, and the cystine transporter, as part of the antioxidant response element, provides a biomarker for OS imaging. A specific radiotracer driven by OS may have value in detection, staging, and therapy

response monitoring (4). Here, we have reported the use of ^{18}F -FASu as a cystine/glutamate analog for monitoring system x_C^- in 3 models of breast cancer. The goal was to evaluate ^{18}F -FASu as an indirect, noninvasive indicator of cellular OS via system x_C^- .

Using a transduced HEK::xCT cell line, we established a positive control to help examine the specificity of ^{18}F -FASu toward system x_C^- . HEK::xCT showed much higher ^{18}F -FASu cellular uptake than did HEK wild-type ($P < 0.0001$). Studies on mice bearing both HEK::xCT and HEK wild-type tumors demonstrated significantly higher uptake in HEK::xCT than in HEK wild-type ($P = 0.0086$).

We also studied tracer specificity using cell-based uptake experiments and inhibition assays in a triple-negative breast

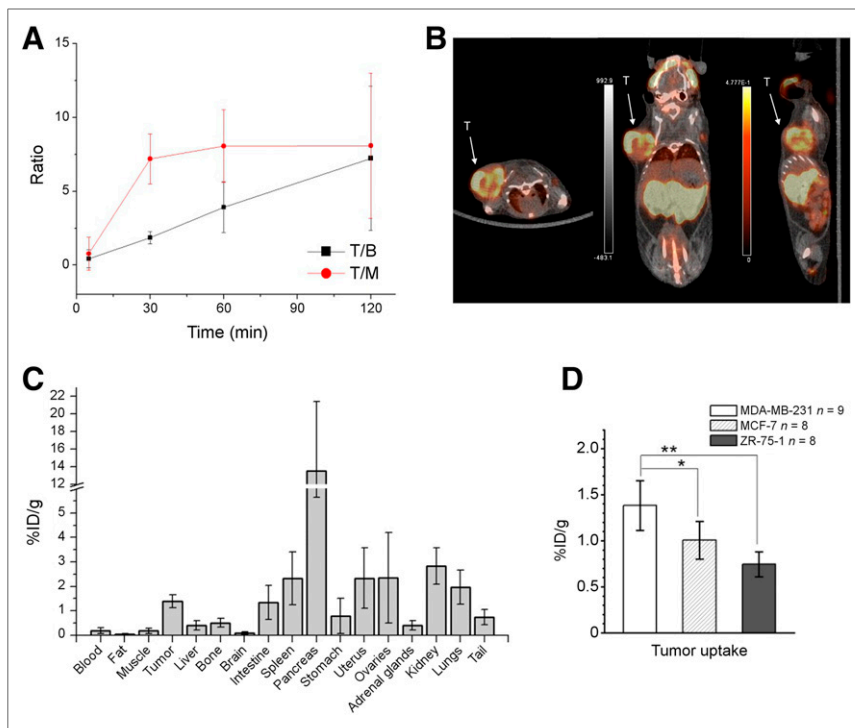


FIGURE 5. ^{18}F -FASu PET image and biodistribution in breast cancer tumor-bearing mice. (A) Tumor-to-blood and tumor-to-muscle uptake ratio at various time points in MDA-MB-231 tumor-bearing mice. (B) PET imaging of MDA-MB-231 tumor-bearing mouse at 2 h after injection (fused PET/CT axial, coronal, and sagittal slices). (C) Biodistribution in MDA-MB-231 tumor-bearing mice at 2 h after injection. (D) Comparison of tumor uptake in mice bearing MDA-MB-231, MCF-7, and ZR-75-1 tumors at 2 h after injection. * $P = 0.0058$. ** $P < 0.0001$. T = tumor; T/B = tumor-to-blood ratio; T/M = tumor-to-muscle ratio.

cancer cell line, MDA-MB-231. We observed strong inhibition with L-Cys and L-Glu, two natural substrates of system x_C^- , and significant blocking in the presence of sulfasalazine, a known x_C^- inhibitor. There was no inhibition with D-Asp, L-Leu, L-Ser, or BCH, establishing a negligible substrate role for systems L, A, ACS, B⁰, B⁰⁺, and excitatory amino acid transporter activity.

Additional evidence for specificity came from xCT siRNA knockdown studies that showed reduced tracer uptake when cells were treated with anti-xCT siRNA but not with control siRNA. Finally, under conditions in which OS was induced by DEM, we showed that both intracellular glutathione levels and tracer uptake increase with increased DEM dose. The results indicate a positive correlation between cellular OS and ^{18}F -FASu uptake.

We then applied this tracer to assess system x_C^- in 3 different breast cancer cell lines: ZR-75-1 (ER+/PR+/Her2-), MCF-7 (ER+/PR+/Her2-), and MDA-MB-231 (ER-/PR-/Her2-). We found that the triple-negative breast cancer cell line MDA-MB-231 had higher tracer uptake in vitro and higher tumor uptake in vivo. These results further confirm that ^{18}F -FASu can be used as a noninvasive indicator of system x_C^- activity. These results also validate system x_C^- as a biomarker across different breast cancer subtypes. Although ^{18}F -FDG PET has shown its potential in diagnosing breast cancers, variable sensitivity and specificity, along with inconsistencies for small and low-grade lesions, limit its clinical use in the detection of these tumors (26). Because ^{18}F -

FDG is not used for primary breast cancer detection, alternative biomarkers could provide a different perspective to meet the challenges of diagnosing and monitoring breast cancer subtypes. Previous studies have established triple-negative breast cancer as having higher xCT expression and higher cystine consumption, which support the potential utility of this biomarker for xCT PET in clinical breast cancer management (8).

^{18}F -(4S)-4-(3- ^{18}F -fluoropropyl)-L-glutamate is another system x_C^- PET tracer that has been used in patients with non-small cell lung, breast, and liver cancers (19,27). Although similar in target, these two tracers maintain key differences in their respective structural arrangement of the carbon backbone. ^{18}F -(4S)-4-(3- ^{18}F -fluoropropyl)-L-glutamate maintains a 4-bond separation between carboxyl groups, whereas ^{18}F -FASu has 7, making the latter closer in structural orientation to cystine. We presume that the affinity and specificity of the two tracers toward system x_C^- will be different, and work comparing these tracers is currently under way to establish their respective value as specific xCT transporter imaging agents.

CONCLUSION

The data within support our hypothesis for using ^{18}F -FASu as a tracer to monitor system x_C^- in vivo. ^{18}F -FASu is a specific tracer for system x_C^- in 3 separate human breast cancer models. Further studies are under way to better understand the effect of optical purity on tumor uptake and image quality. Experiments are also under way to compare ^{18}F -FASu with ^{18}F -FDG (OS vs. glucose metabolism) and ^{18}F -(4S)-4-(3- ^{18}F -fluoropropyl)-L-glutamate (structurally unique x_C^- tracers). We expect that the ability to assess x_C^- via PET will contribute to an understanding of its role in disease and will speed the development of interventions that moderate OS-related disease processes.

DISCLOSURE

Financial support was received from CIHR (201403COP, 329895). Michael Rishel, Bruce Johnson, and Jack Webster were supported by NIH 5R01EB014250-04. TRIUMF receives federal funding via a contribution agreement with the National Research Council of Canada. Bruce Johnson and Michael Rishel are employed by GE Global Research. No other potential conflict of interest relevant to this article was reported.

ACKNOWLEDGMENTS

We thank the TRIUMF TR13 cyclotron operators, the BC Cancer Research Centre PET imaging staff, Lily Southcott, Iulia Dude, and Sofya Langman for their technical help.

REFERENCES

- Nagano O, Okazaki S, Saya H. Redox regulation in stem-like cancer cells by CD44 variant isoforms. *Oncogene*. 2013;32:5191–5198.
- Dayem AA, Choi HY, Kim JH, Cho SG. Role of oxidative stress in stem, cancer, and cancer stem cells. *Cancers (Basel)*. 2010;2:859–884.
- Nguyen T, Nioi P, Pickett CB. The Nrf2-antioxidant response element signaling pathway and its activation by oxidative stress. *J Biol Chem*. 2009;284:13291–13295.
- Conrad M, Sato H. The oxidative stress-inducible cystine/glutamate antiporter, system x_c^- : cystine supplier and beyond. *Amino Acids*. 2012;42:231–246.
- Bridges RJ, Natale NR, Patel SA. System x_c^- cystine/glutamate antiporter: an update on molecular pharmacology and roles within the CNS. *Br J Pharmacol*. 2012;165:20–34.
- Ishii T, Sato H, Miura K, Sagara J, Bannai S. Induction of cystine transport activity by stress. *Ann N Y Acad Sci*. 1992;663:497–498.
- Lo M, Wang YZ, Gout PW. The x_c^- cystine/glutamate antiporter: a potential target for therapy of cancer and other diseases. *J Cell Physiol*. 2008;215:593–602.
- Timmerman LA, Holton T, Yuneva M, et al. Glutamine sensitivity analysis identifies the xCT antiporter as a common triple-negative breast tumor therapeutic target. *Cancer Cell*. 2013;24:450–465.
- Yoshikawa M, Tsuchihashi K, Ishimoto T, et al. xCT inhibition depletes CD44v-expressing tumor cells that are resistant to EGFR-targeted therapy in head and neck squamous cell carcinoma. *Cancer Res*. 2013;73:1855–1866.
- Dai L, Cao YY, Chen YH, Parsons C, Qin ZQ. Targeting xCT, a cystine-glutamate transporter induces apoptosis and tumor regression for KSHV/HIV-associated lymphoma. *J Hematol Oncol*. 2014;7:30.
- Doxsee DW, Gout PW, Kurita T, et al. Sulfasalazine-induced cystine starvation: potential use for prostate cancer therapy. *Prostate*. 2007;67:162–171.
- Lay JD, Hong CC, Huang JS, et al. Sulfasalazine suppresses drug resistance and invasiveness of lung adenocarcinoma cells expressing AXL. *Cancer Res*. 2007;67:3878–3887.
- Narang VS, Pauletti GM, Gout PW, Buckley DJ, Buckley AR. Sulfasalazine-induced reduction of glutathione levels in breast cancer cells: enhancement of growth-inhibitory activity of doxorubicin. *Chemotherapy*. 2007;53:210–217.
- Pham AN, Blower PE, Alvarado O, Ravula R, Gout PW, Huang Y. Pharmacogenomic approach reveals a role for the x_c^- cystine/glutamate antiporter in growth and Celestrol resistance of glioma cell lines. *J Pharmacol Exp Ther*. 2010;332:949–958.
- Müerköster S, Arlt A, Witt M, et al. Usage of the NF-kappa B inhibitor sulfasalazine as sensitizing agent in combined chemotherapy of pancreatic cancer. *Int J Cancer*. 2003;104:469–476.
- Qin Z, Freitas E, Sullivan R, et al. Upregulation of xCT by KSHV-encoded microRNAs facilitates KSHV dissemination and persistence in an environment of oxidative stress. *PLoS Pathog*. 2010;6:e1000742.
- Webster JM, Morton CA, Johnson BF, et al. Functional imaging of oxidative stress with a novel PET imaging agent, F-18-5-fluoro-L-aminosuberic acid. *J Nucl Med*. 2014;55:657–664.
- Karihtala P, Kauppila S, Soini Y, Arja-Jukkola-Vuorinen. Oxidative stress and counteracting mechanisms in hormone receptor positive, triple-negative and basal-like breast carcinomas. *BMC Cancer*. 2011;11:262.
- Baek S, Choi CM, Ahn SH, et al. Exploratory clinical trial of (4S)-4-(3-[18 F] fluoropropyl)-L-glutamate for imaging xCT transporter using positron emission tomography in patients with non-small cell lung or breast cancer. *Clin Cancer Res*. 2012;18:5427–5437.
- Bannai S. Induction of cystine and glutamate transport activity in human-fibroblasts by diethyl maleate and other electrophilic agents. *J Biol Chem*. 1984;259:2435–2440.
- Hosoya K, Tomi M, Ohtsuki S, et al. Enhancement of L-cystine transport activity and its relation to xCT gene induction at the blood-brain barrier by diethyl maleate treatment. *J Pharmacol Exp Ther*. 2002;302:225–231.
- Sasaki H, Sato H, Kuriyama-Matsumura K, et al. Electrophile response element-mediated induction of the cystine/glutamate exchange transporter gene expression. *J Biol Chem*. 2002;277:44765–44771.
- Barretina J, Caponigro G, Stransky N, et al. The Cancer Cell Line Encyclopedia enables predictive modelling of anticancer drug sensitivity. *Nature*. 2012;483:603–607.
- Lo M, Ling V, Wang YZ, Gout PW. The x_c^- cystine/glutamate antiporter: a mediator of pancreatic cancer growth with a role in drug resistance. *Br J Cancer*. 2008;99:464–472.
- Kapushesky M, Emam I, Holloway E, et al. Gene Expression Atlas at the European Bioinformatics Institute. *Nucleic Acids Res*. 2010;38:D690–D698.
- Rosen EL, Eubank WB, Mankoff DA. FDG PET, PET/CT, and breast cancer imaging. *Radiographics*. 2007;27(suppl):S215–S229.
- Koglin N, Mueller A, Berndt M, et al. Specific PET imaging of x_c^- transporter activity using a 18 F-labeled glutamate derivative reveals a dominant pathway in tumor metabolism. *Clin Cancer Res*. 2011;17:6000–6011.